



Published in final edited form as:

Clin Cancer Res. 2015 October 15; 21(20): 4642–4651. doi:10.1158/1078-0432.CCR-15-0781.

Treatment with ibrutinib inhibits BTK and VLA-4 dependent adhesion of chronic lymphocytic leukemia cells in vivo

Sarah E. M. Herman^{1,*}, Rashida Z. Mustafa^{1,*}, Jade Jones^{1,2}, Deanna H. Wong¹, Mohammed Farooqui¹, and Adrian Wiestner¹

¹Hematology Branch, National Heart, Lung, and Blood Institute, National Institutes of Health, Bethesda, MD

²Medical Research Scholars Program, National Institutes of Health, Bethesda, MD

Abstract

Purpose—Ibrutinib leads to a transient lymphocytosis in patients with chronic lymphocytic leukemia (CLL) that develops within hours of starting drug and is due to the efflux of cells from lymphoid tissues into the blood. We therefore sought to investigate the *in vivo* effect of ibrutinib on migration and adhesion of CLL cells.

Experimental Design—Patients received single agent ibrutinib (420mg daily) on an investigator-initiated phase 2 trial. Serial blood samples were collected pre-treatment and during treatment for *ex vivo* functional assays.

Results—Adhesion of CLL cells to fibronectin was rapidly (within hours) and almost completely inhibited (median reduction 98% on day 28, $P < 0.001$), while the effect on migration to chemokines was more moderate (median reduction 64%, $P = 0.008$) and less uniform. Although cell surface expression of key adhesion molecules such as CD49d, CD29 and CD44 were modestly reduced, this was only apparent after weeks of treatment. Stimulation of CLL cells from patients on ibrutinib with PMA, which activates PKC independent of BTK, restored the ability of the cells to adhere to fibronectin in a VLA-4 dependent manner. Lastly, the addition of ibrutinib to CLL cells adhered to fibronectin *in vitro* caused the detachment of 17% of the cells, on average; consistent with *in vivo* observations of an increasing lymphocytosis within 4 hours of starting ibrutinib.

Corresponding author: Adrian Wiestner, Hematology Branch, NHLBI, NIH, Bldg. 10, CRC 3-5140, 10 Center Drive 20892-1202 Bethesda, MD phone: +1 (301) 496 5093, fax: +1(301) 496 8396.

*S.E.M.H. and R.Z.M. contributed equally to this work and are co-first authors

Conflicts of Interest: A.W. received research support from Pharmacyclics, Inc. All other authors declare no competing financial interests.

Authors' Contributions

Concept and design: S.E.M. Herman and A. Wiestner

Development of methodology: S.E.M. Herman, R.Z. Mustafa and A. Wiestner

Acquisition of data: S.E.M. Herman, R.Z. Mustafa, J. Jones and D.H. Wong

Analysis and interpretation of data: S.E.M. Herman, R.Z. Mustafa, J. Jones and D.H. Wong

Writing, review and/or revision of manuscript: S.E.M. Herman, R.Z. Mustafa, J. Jones, D.H. Wong, M. Farooqui and A. Wiestner

Study supervision: M. Farooqui

Conclusions—Inhibition of BTK and VLA-4 dependent adhesion of CLL cells to stroma and stromal components provides a mechanistic explanation for the treatment-induced lymphocytosis and may reduce CD49d-dependent pro-survival signals in the tissue microenvironment.

Keywords

ibrutinib; adhesion; lymphocytosis; BTK and VLA-4

Introduction

CLL is a malignancy of mature auto-reactive B-cells (1, 2). The tumor microenvironment in secondary lymphoid tissues and the bone marrow plays a key role in the pathogenesis of the disease (3–5). This is underscored by the observation that CLL cells undergo apoptosis *in vitro* unless surrogates of survival signals found in the tumor microenvironment are provided. Further, Herishanu et al. presented direct *in vivo* evidence that CLL cells are activated through the B-cell Receptor (BCR) in the lymph node microenvironment (4). The BCR signaling pathway has emerged as a pivotal pathway in the pathogenesis of CLL and as a target for novel therapies (6–8). Bruton's tyrosine kinase (BTK), a cytoplasmic TEC kinase, couples BCR activation to intracellular calcium release and NF- κ B signaling (9). BTK plays an essential role in B-cells as demonstrated by the severe defect in B-cell development due to loss of function mutations in this kinase in patients with X-linked agammaglobulinemia. Further, deletion of BTK in murine models supports a critical role for BTK in the development and progression of CLL (10, 11)

Ibrutinib, an orally active covalent BTK inhibitor, was recently approved in the USA and Europe for the treatment of patients with CLL who have received at least one prior therapy as well as of previously-untreated patients who carry a deletion of chromosome band 17p13.1. Several clinical trials have shown that single-agent ibrutinib is well tolerated and can induce objective clinical responses in CLL; including in patients with high risk disease features (12–14). Even as a single agent, ibrutinib induced durable responses in CLL patients with TP53 aberrations, including deletion 17p13.1 (del(17p)) and TP53 mutation, contrasting with the inferior responses and relatively early relapses when these high risk patients are treated with chemoimmunotherapy (14). In a randomized phase 3 study of ibrutinib versus ofatumumab for relapsed or refractory CLL, patients treated with ibrutinib had a 78% reduction in the risk of tumor progression or death compared to patients in the ofatumumab arm (15).

A transient increase in lymphocytosis is commonly observed when treatment with ibrutinib or other BCR-directed kinase inhibitors is initiated (13, 16). In our investigator-initiated phase 2 study of ibrutinib in CLL, the average peak increase in the absolute lymphocyte count was greater than 65%, with more than 40% of patients reaching the peak on or before day 2 of therapy and 78% by day 28 (16). Additionally, we found that the ibrutinib-induced increase in lymphocytosis, at least early on treatment, is due to the release of tumor cells from the tissue compartment into the peripheral blood (16). This is considered to be an important drug effect as the microenvironment protects tumor cells from apoptosis through various stimuli such as chemokines, cytokines, and direct interactions with accessory cells

and adhesion molecules (3, 17). The hypothesis that ibrutinib, through a disruption of these tumor-microenvironment interactions, could sensitize the cells to cytotoxic or antibody therapy is currently being investigated in clinical trials.

In vitro studies with ibrutinib have demonstrated reductions in both CLL cell migration and adhesion; key mechanisms in the trafficking of cells between the peripheral blood and secondary lymphoid tissues. It has been previously shown that treatment with 1 μ M ibrutinib inhibits CLL cell chemotaxis toward the chemokines CXCL12, CXCL13 and CCL19 (18, 19). Additionally, *in vitro* treatment with ibrutinib diminishes BCR-activated CLL cell adhesion to fibronectin and vascular cell adhesion molecule-1 (VCAM-1) (18). However, data on drug effects *in vivo* are limited. Within the microenvironment, integrins play a pivotal role in establishing contact of CLL cells with their surroundings and other cells (3, 17). A molecule of central importance for these tumor-microenvironment interactions is CD49d (integrin α 4) which heterodimerizes with CD29 (integrin β 1) to form VLA-4 (20, 21). VLA-4 on CLL cells binds to fibronectin and VCAM-1 in the tissue compartments. CD49d is one of the most powerful prognostic markers in CLL; with high expression of CD49d on CLL cells identifying a more aggressive disease subset with inferior survival (22, 23). To characterize the *in vivo* drug effect on cell adhesion and migration we performed functional assays *ex vivo* using peripheral blood samples collected from CLL patients treated on an investigator-initiated phase 2 single agent ibrutinib trial.

Materials and Methods

Patient samples

This clinical trial of ibrutinib was registered at clinicaltrials.gov as NCT01500733. Patients with CLL or SLL who were either over the age of 65 or had TP53 aberrations were enrolled from December 2011 to January 2014. A total of 86 patients were enrolled, 30 of which were evaluated in this study. A few (n=4) untreated CLL patients enrolled on a natural history study (registered as NCT00923507 at clinicaltrials.gov) were also included in this study. For each set of analyses, 7–20 patients were evaluated; Supplementary Table S1 denotes which patients were analyzed in each experiment. Written informed consent was obtained in accordance with the Declaration of Helsinki, applicable federal regulations, and requirements of local institutional review boards. Peripheral blood samples were obtained pre-treatment (Pre) and on days 2 (after one dose of drug), 14, and 28 of ibrutinib treatment. Peripheral blood mononuclear cells (PBMCs) were isolated by density-gradient centrifugation (Ficoll Lymphocyte Separation Media; ICN Biomedicals) and viably frozen in 90% fetal bovine serum (FBS), 10% dimethyl sulfoxide (DSMO) (Sigma) in liquid nitrogen. Plasma supernatant from bone marrow aspirates was collected at baseline, prior to initiation of treatment. Clinical patient characteristics are summarized in Supplementary Table S2.

Chemotaxis assay

Chemotaxis assays across polycarbonate Transwell inserts were performed as previously described (24). Briefly, 10⁶ CLL PBMCs in AIM-V medium (Gibco) were transferred into the top chambers of Transwell culture inserts (Corning Incorporated) with a diameter of 6.5

mm and a pore size of 5 μm . Filters were then placed into wells containing medium (control), medium with 200 ng/mL CXCL12 and 100 ng/mL CCL19 (Prospec) or a mixture of 50% medium and 50% bone marrow supernatant collected pre-treatment. Where indicated, cells were pre-incubated with 1 μM ibrutinib (Sellekchem) *in vitro* for 1 hour. CLL PBMCs were allowed to migrate for 3 hours at 37°C. Migrated cells in the lower chamber were collected, stained with CD19 and CD3 and counted using AccuCount blank particles (Spherotech) as previously described (25). The migration index was determined by subtracting the percent migration of the medium control from the percent migration of the chemottractant wells and normalizing. Migration experiments were performed in triplicate plates; results are reported as the average.

Flow cytometry

Cells were stained as previously described (26) with the following antibodies: anti- CD19-APC and CD3-FITC and in select experiments one of the following PE conjugated antibodies: IgG1-isotype control, anti-CXCR4, CCR7, CD38, CD49d, CD29 and CD44 (BD Biosciences). Cells were analyzed on a FACS Canto II flow cytometer (BD Biosciences) using FACS-DIVA 6.1.1 and FlowJo (Version 10, TreeStar).

Ex vivo adhesion assay

PBMCs were labeled with carboxyfluorescein diacetate succinimidyl ester (CFSE; Invitrogen). PBMCs were plated at 10^7 cells/mL in 500 μL into 24-well fibronectin coated plates (Corning Incorporated). Where indicated, cells were incubated with 1 μM ibrutinib, 500nM fipristone (VLA-4 antagonist; MedChem Expression), 50ng/mL Phorbol 12-myristate 13-acetate (PMA; Sigma), 10 $\mu\text{g/mL}$ αCD18 (Abcam Inc.), 10 $\mu\text{g/mL}$ αCD29 (R&D Systems) or 10 $\mu\text{g/mL}$ αCD49d (LifeSpan BioSciences, Inc.) for 1 hour at 37°C. The plates were centrifuged at 400 \times g for one minute and cells were left to adhere for 1 hour at 37°C. Non-adhered cells were removed by washing three times with PBS (Lonza). Wells were imaged using the EVOS fl microscope (Advanced Microscopy Group). Quantification of the number of adhered CLL PBMCs was done using the Image J software (NIH). Experiments were performed in duplicate plates with 4–6 images collected per plate; results are reported as the median cell count per visual field.

Stromal cell adhesion assay

HS5 bone marrow stromal cells (ATCC[®], CRL-11882[™]; passages 5–10) were cultured for two days until 95% confluency in 25cm² culture flasks. HS5 cells were routinely evaluated for changes in cell viability and morphology. CFSE labeled PBMCs were added at 8×10^6 cells/mL in 3mL to the flasks and allowed to adhere for 2 hours at 37°C. Where indicated, cells were incubated with 1 μM ibrutinib for 1 hour. Flasks were washed three times and imaged using EVOS fl microscope and the number of adhered CLL PBMCs was quantified using the Image J software.

Release assay

CFSE labeled PBMCs obtained pre-treatment were adhered to 24-well fibronectin coated plates for 16 hours at 37°C. Non-adhered cells were removed and the plates were washed

three times with PBS. 1 μ M ibrutinib was added for 1 hour at 37°C. The plates were washed three times with PBS, with cells released into the media collected and counted using the Vi-Cell XR (Beckman Coulter). Wells were imaged using the EVOS fl microscope and the number of adhered CLL PBMCs was quantified using the Image J software.

Results

Ibrutinib inhibits migration of CLL cells

To determine the effect of ibrutinib on cellular migration in CLL PBMCs *ex vivo*, we used standard transwell migration assays. To validate our method respective to previously published *in vitro* data, we first evaluated the effect of *in vitro* treatment of CLL cells on migration towards two important chemokines, CXCL12 and CCL19, using, as in the previous reports, a dose of 1 μ M ibrutinib (18, 19). As expected, there was a modest but significant reduction in the migration of ibrutinib treated CLL cells towards the chemokine mixture (median change -33%, IQR: -2 to -59, n=12, $P=0.04$, Supplementary Fig. S1A), although 3/12 patients did not show a reduction in cellular migration after ibrutinib treatment. In contrast, we did not observe a significant inhibition of T-cell migration (median change -8%, IQR: +24 to -21, n=12, $P=0.28$, Supplementary Fig. S1A). We next evaluated the migratory ability of cells collected pre-treatment compared to those collected from patients treated for 28 days with ibrutinib, the time point at which more than 75% of patients reached their peak ALC. This was done in all 12 patients evaluated *in vitro*, plus an additional three patients where samples were available (Supplemental Table S1). There was a significant reduction in migration of CLL cells obtained during treatment with ibrutinib compared to pre-treatment (median change -65%, IQR: -33 to -97, n=12, $P=0.007$, Fig. 1A), albeit with considerable inter-patient variability. In fact, in one of fifteen patients tested there was a marked increase in migration (Fig. 1A). Key prognostic markers, such as del(17p), *IGHV* mutational status and prior treatment history could not account for the observed inter-patient variability (n=15, Supplementary Fig. S1B). Notably, a majority of the evaluated patients demonstrated a superior inhibition of migration after *in vivo* treatment compared to what was observed *in vitro*. To determine if the superior *in vivo* effect could be attributed to a reduction in chemokine receptors overtime on drug we evaluated the expression of CXCR4 and CCR7 (the receptors for CXCL12 and CCL19, respectively). Baseline expression of these chemokine receptors is summarized in Supplementary Table S3. We found that there was a significant reduction in the expression of CCR7 on ibrutinib (median change -38%, IQR: -21 to -44, n=13, $P<0.001$, Fig. 1B). In contrast, expression of CXCR4 was not significantly reduced (median change -14%, IQR: +46 to -30, n=13, $P=0.89$, Fig. 1B). In contrast to what was observed with CLL cells, there was no consistent effect on T-cell migration (median change +41%, IQR: -9 to +271, n=15, $P=0.08$, Fig. 1A). In fact, we found that 75% of evaluated patients demonstrated an increase in T-cell migration on ibrutinib.

Because the tumor microenvironment contains a mix of many different factors in addition to CXCL12 and CCL19, we used the plasma supernatant from bone marrow aspirates collected pre-treatment as a more physiological chemoattractant. Indeed, a mixture of equal amounts of bone marrow supernatant and medium induced CLL cell migration similarly, if not better,

than that observed with CXCL12/CCL19 (data not shown). Compared to cells obtained pre-treatment, cells collected after 28 days on ibrutinib demonstrated a reduction in migration towards patient matched bone marrow supernatant (median change -44%, IQR: -22 to -96, n=7, $P=0.02$, Fig. 1C). Together these data show that ibrutinib reduces the migration of CLL cells towards a variety of chemoattractants; however, the effect on migration is moderate and not apparent in all patients, despite a rise in ALC on treatment in all patients contributing cells for analysis.

Ibrutinib inhibits CLL cell adhesion to fibronectin and stromal cells

To determine the effect of ibrutinib treatment on cell adhesion we chose a functional assay, utilizing fibronectin coated plates to model tumor-stromal interactions in the tissue microenvironment. We validated the performance of the assay using CFSE labeled PBMCs (CLL cell content 88–99%, Supplementary Table S4), either treated with 1 μ M ibrutinib or left untreated, and allowed them to adhere to a fibronectin-coated plate. After extensive washing, we quantified the number of adhered cells and found that there was a modest, but significant reduction in cell adhesion to fibronectin after ibrutinib treatment *in vitro*, confirming what has been previously reported (18) (median change -35%, IQR: -18 to -63, n=11, $P=0.002$, Supplementary Fig. S2A–B).

Next we determined the effect of *in vivo* ibrutinib treatment using PBMCs collected from patients pre-treatment and after 28 days on ibrutinib. The percentage of CLL cells at all evaluated time points ranged from 88–99% (Supplementary Table S4). Figure 2A depicts representative microscopic images demonstrating the inability of CLL cells from patients treated with ibrutinib to adhere to fibronectin. This dramatic effect was seen in all patients evaluated (median change -98%, IQR: -91 to -100, n=13, $P<0.001$, Fig. 2B). Because the onset of ibrutinib-induced lymphocytosis is virtually immediate and in many patients peaked within days (16), we also analyzed cells obtained after just one dose of ibrutinib (day 2). Even at this early time-point, adhesion was significantly reduced (median change -68%, IQR: -40 to -85, n=10, $P=0.002$; Fig. 2C) and was further reduced with continued treatment (n=8, Fig. 2D). We again found that key prognostic markers could not account for the observed inter-patient variability (n=10, Supplementary Fig. S2C). As fibronectin is only one of the many molecules that can facilitate adhesion, we repeated our analyses using the Hs5 stromal cell line. We again found that there was only a modest reduction in adhesion after ibrutinib treatment *in vitro* (median change -14%, IQR: -6 to -29, n=9, $P=0.004$, Supplementary Fig. S3A); with a more substantial reduction observed in cells obtained from patients after 28 days on ibrutinib (median change -20%, n=11, $P=0.005$, IQR: -5 to -30, Supplementary Fig. S3B–C). In summary, treatment with ibrutinib consistently abrogated adhesion of CLL cells to fibronectin and significantly reduced their ability to adhere to stromal cells.

Ibrutinib treatment leads to a release of adhered cells

Having demonstrated that circulating CLL cells from the blood of patients being treated with ibrutinib have a defect in cell adhesion, we sought to determine whether ibrutinib could also detach CLL cells already firmly adhered to solid supports. To address this question, we evaluated CLL PBMCs collected pre-treatment and from untreated CLL patients enrolled on

a natural history study (Supplemental Table S1). CLL PBMCs were allowed to adhere to fibronectin-coated plates overnight. The next day the plates were washed extensively to remove all cells not firmly attached, and then incubated with 1 μ M ibrutinib for 1 hour. Micrographs in Figure 3A show results of two representative experiments utilizing samples collected pre-ibrutinib. Overall, there was a moderate, but uniform decrease in the number of adherent cells in plates treated with ibrutinib compared to controls (median change -17%, IQR: -6 to -27, n=11, $P=0.002$, Fig. 3B). Conversely, treatment with ibrutinib lead to a significant increase in the number of cells released into the cell culture supernatant (median change +22%, IQR: +1 to +78, n=11, $P=0.02$, Fig. 3C). Collectively, these data show that ibrutinib can detach and mobilize cells that are adhered to fibronectin; however, only a minor fraction of the total cells are being released.

Ibrutinib modestly reduces expression of adhesion molecules that bind fibronectin

Next we sought to investigate the mechanisms responsible for the observed decrease in cellular adhesion on ibrutinib in a subset of patients. We first analyzed expression of the most common adhesion molecules known to bind to fibronectin. In particular, we evaluated CD44, which binds to the COOH-terminal heparin binding domain, and very late antigen-4 (VLA-4), a heterodimer of integrin α 4 (CD49d) and integrin β 1 (CD29), which binds to the IIIICS (V) CS1 region and the EIIIA domain of fibronectin (27, 28). Baseline expression of these key integrins is summarized in Supplementary Table S3. Figure 4A summarizes the average change (day 28 compared to pre-treatment) in the mean fluorescence intensity (MFI) of a given adhesion molecule and in the fraction of CLL cells expressing it above isotype control. The percentage of CLL cells expressing CD49 (median change -2%, IQR: 0 to -18) and CD29 (median change -7%, IQR: 0 to -27) decreased significantly on ibrutinib compared to controls (n=20, $P=0.02$ and $P=0.009$, respectively, Fig. 4A). While the percentage of cells expressing CD44 did not change, the MFI of CD44 was significantly reduced after 28 days on ibrutinib (median change -9%, IQR: +5 to -19, n=19, $P=0.03$, Fig. 4A). This apparent discrepancy is due to the very high expression of CD44 at baseline so that even in samples with a substantial reduction, CD44 remained expressed on almost all CLL cells after treatment. The changes in expression of the adhesion molecules in individual patients are summarized in Figure 4. In 12 of 20 patients (60%), CLL cells, obtained at baseline, expressed CD49d; of these, 7 (58%) showed a reduction on ibrutinib (Fig. 4B). Similarly, CD29, expressed in all patients at baseline, decreased in 12 of 20 patients (60%) on treatment (Fig. 4C). Lastly, the expression level of CD44 decreased in 10 of 19 evaluated patients (60%) after 28 days of *in vivo* ibrutinib treatment (Fig. 4D). In summary, ibrutinib modestly reduced the expression of adhesion molecules; however this occurred in only a little more than half of the evaluated patients.

Adhesion of CLL cells is equally reduced by ibrutinib and VLA-4 blockade

As VLA-4 has been demonstrated to be a key molecule in facilitating binding to fibronectin, we tested the importance of VLA-4 for CLL cell adhesion using the small molecule α 4 β 1-integrin antagonist fiategrast. A dose titration of fiategrast was performed from 100nM to 10 μ M; 500nM was determined to be the lowest optimal concentration for inhibition of CLL cell adhesion to fibronectin (data not shown). Treatment of CLL PBMCs with fiategrast *in vitro* significantly reduced CLL cells adhesion to fibronectin (median change -32%, IQR:

–13 to –44, $n=15$, $P=0.001$, Fig. 5A). To further delineate if CD49d is the key alpha integrin important for CLL adhesion to fibronectin, we treated CLL PBMCs with blocking antibodies against integrin $\alpha 4$ and $\beta 1$ separately. The blockade of integrin $\alpha 4$ (CD49d) inhibited cellular adhesion significantly (median change –23%, IQR: –10 to –60, $n=11$, $P<0.001$, Fig. 5B), while the anti-integrin $\beta 1$ (CD29) antibody had no consistent effect (Fig. 5B). Notably, the degree of inhibition achieved with ibrutinib and anti-CD49d was highly correlated ($R=0.90$, $n=11$, $P<0.001$; Fig. 5C). As a control we used a blocking antibody against integrin $\beta 2$ (CD18), an adhesion molecule that does not bind fibronectin, and saw no effect ($n=11$, Supplementary Fig. S4). Thus, both CD49d and BTK are important for CLL cell adhesion and inhibition of either molecule inhibits adhesion of CLL cells to a similar degree.

The adhesion defect induced by ibrutinib is at least partially VLA-4 dependent

VLA-4 dependent cell adhesion of B-cells is increased in response to BCR signaling through PKC activation (29, 30). We therefore tested whether activation of PKC with PMA, which is independent of BTK (31), would restore the ability of ibrutinib treated cells to adhere through VLA-4. As shown in Figure 2, CLL cells collected from patients on ibrutinib had an adhesion defect. Stimulation of these cells with PMA *in vitro* induced a significant increase, or recovery, in cell adhesion ($n=12$, $P<0.001$, Fig. 6A). Despite pronounced inter-patient variability in the recovery of adhesion with PMA (IQR: +9 to +87% of control), there was a significant correlation between the abolishment of adhesion by ibrutinib and the recovery by PMA ($R=0.76$, $n=12$, $P=0.004$, data not shown). Blocking VLA-4 with firsategrast abolished the PMA-mediated recovery in the ability of ibrutinib treated cells to adhere to fibronectin (median change –65%, IQR: –38 to –94, $n=11$, $P<0.001$, Fig. 6B). Notably, firsategrast did not further reduce the ability of CLL cells collected from patients on ibrutinib to adhere to fibronectin, indicating maximal inhibition of VLA-dependent adhesion of CLL cells is achieved with ibrutinib ($n=11$, $P=0.34$, Fig. 6B). Therefore, ibrutinib, through inhibition of BTK, results in the blockade of VLA-4 activity, reducing the ability of cells to adhere.

Discussion

Treatment-induced lymphocytosis, the transient increase in circulating tumor cells at the initiation of treatment of CLL patients with kinase inhibitors, is a hallmark of these targeted agents (13, 16, 32). As we previously reported, the onset of ibrutinib-induced lymphocytosis is virtually immediate and, at least initially, due to an efflux of cells from the lymph node into the peripheral blood (16). *In vitro* ibrutinib can disrupt several survival pathways, including cell migration and adhesion that are important for tumor-microenvironment interactions (18, 19, 33). Here we investigated the effects of ibrutinib *in vivo* by analyzing CLL cells obtained from patients treated with single agent ibrutinib. The most striking finding was that circulating CLL cells from patients having received ibrutinib for 28 days showed a near complete loss in their ability to adhere to fibronectin. Notably, this effect was ubiquitous, occurring in all samples studied, and already apparent after just one dose of drug, consistent with the timing of the lymphocytosis. Inhibition of cell adhesion appears to be a direct effect of ibrutinib as it manifested within hours of the first dose and was readily reversible in cells stimulated with PMA, which activates PKC independent of BTK (29, 31).

While we also observed some reduction in the expression of the adhesion molecules CD29, CD44 and CD49d, these changes were minimal, did not occur in all patients and were only apparent at later time points, suggesting that down-modulation of adhesion molecules is not the primary reason for the observed adhesion defect. Additionally, we also demonstrated a reduction in cell migration in samples obtained after 28 days of ibrutinib treatment; however, this effect was more variable and not seen in all patients.

BCR signaling is known to activate integrin dependent cell adhesion referred to as inside-out activation (34, 35). In response to BCR activation, VLA-4 is released from a constrained position allowing the formation of VLA-4 clusters with enhanced avidity (29). Two sets of experiments indicate that ibrutinib abrogates VLA-4-dependent adhesion of CLL cells, consistent with inhibition of inside-out activation. First, pre-treatment CLL cell adhesion to fibronectin was inhibited both by the small molecule VLA-4 antagonist fiategrast as well as by a blocking antibody against integrin $\alpha 4$ (CD49d), one of the heterodimer components of VLA-4. However, in cells treated with ibrutinib there was no further reduction in cell adhesion using these inhibitors, suggesting that ibrutinib already completely blocked VLA-4 dependent adhesion. Second, while PMA rapidly restored adhesion of ibrutinib treated CLL cells, this effect was completely inhibited by fiategrast, indicating that reactivation of inside-out activation downstream of BTK restores cell adhesion in a VLA-4 dependent manner.

CD49d has been referred to as the master regulator of tumor microenvironmental interactions in CLL by virtue of its regulation of many signaling pathways important to CLL cell proliferation and survival (5). CD49d may be important for keeping CLL cells localized to proliferation centers, as CD49d was found to be up-regulated in the proliferative subset of peripheral blood CLL cells (CXCR4^{dim}CD5^{bright}) (36). Additionally, CD49d has been demonstrated to be a critical regulator of lymphocyte migration (37). The survival effect provided to CLL cells after ligation of CD49d has been shown to be due to BCR-dependent and -independent mechanisms, which include up-regulation in anti-apoptotic proteins such as BCL-2 (with subsequent decreases in BAX), increases in MMP-9 leading to activation of LYN, activation of SYK and PI3K signaling and downstream activation of NF- κ B transcription factors (5, 38–40). Through inhibition of VLA-4 activation, ibrutinib may also interfere with the protective effects mediated by CD49d dependent tumor-microenvironment interactions, including pro-survival and proliferation signals. This is supported by the fact that patients with CD49d^{hi} CLL cells, who have a decreased median overall survival compared to those with CD49d^{lo} CLL cells, have demonstrated increased sensitivity to ibrutinib *in vitro* (23). Additionally, as shown previously, the proliferation of CLL cells in lymph node and bone marrow of patients on ibrutinib is virtually completely inhibited (41).

While the ability of ibrutinib treated CLL cells to adhere to stromal cells was also reduced this was not as pronounced as for fibronectin, suggesting that interactions with the extracellular matrix are more sensitive to the inhibitory effect of ibrutinib than cell-cell interactions. Also an important distinction is that while CLL cells in the blood of patients on ibrutinib almost completely lost their ability to adhere to fibronectin, ibrutinib was only modestly effective in releasing cells already adhered. These observations are consistent with the clinical impression that only a fraction of CLL cells in secondary lymphoid tissues are

mobilized into circulation by ibrutinib, and persistent lymphadenopathy and residual disease in the bone marrow is apparent even after many months of treatment in a subset of patients (14, 16, 42). Therefore, the cells circulating in the peripheral blood during treatment with ibrutinib may be enriched for cells that have strong inhibition in adhesion, while the cells retained in the lymph node may be less affected. Whether the retention of cells in the microenvironment is due to CD49d- or BTK-independent mechanisms still remains to be determined.

Therapeutics that inhibit chemokine signaling and migration (such as plerixafor) and integrin-dependent adhesion and cell trafficking (such as natalizumab and finategrast) mobilize B-cells from the secondary lymphoid tissues into the peripheral blood (43, 44). It has been hypothesized that these agents, by dislocating tumor cells out of protective microenvironmental niches, could synergize with chemotherapeutic agents and monoclonal antibodies (43, 45, 46). Notably, ibrutinib not only combines inhibition of migration and adhesion but also directly inhibits the pro-survival effects of BCR and possibly CD49d mediated signaling in CLL. Thus, ibrutinib may potentially sensitize CLL cells to existing treatment modalities, which could lead to better overall responses. This hypothesis is currently being tested in ongoing clinical trials (47–50).

Supplementary Material

Refer to Web version on PubMed Central for supplementary material.

Acknowledgements

We thank our patients for participating and donating the blood and tissue samples to make this research possible. We thank Susan Soto, Ajunae Wells and Janet Valdez for assistance in the clinic. We acknowledge Pharmacyclics, Inc. for providing study drug and reviewing the manuscript. A. Wiestner and this work were supported by the Intramural Research Program of the National, Heart, Lung and Blood Institute, the National Institutes of Health. J. Jones was supported by the NIH Medical Research Scholars Program, a public-private partnership supported jointly by the NIH and generous contributions to the Foundation for the NIH from Pfizer Inc, The Leona M. and Harry B. Helmsley Charitable Trust, and the Howard Hughes Medical Institute, as well as other private donors.

Research support: This research was supported by the Intramural Research Program of the National, Heart, Lung and Blood Institute

References

1. Caligaris-Cappio F, Ghia P. Novel insights in chronic lymphocytic leukemia: are we getting closer to understanding the pathogenesis of the disease? *J Clin Oncol.* 2008; 26:4497–4503. [PubMed: 18662968]
2. Duhren-von Minden M, Ubelhart R, Schneider D, Wossning T, Bach MP, Buchner M, et al. Chronic lymphocytic leukaemia is driven by antigen-independent cell-autonomous signalling. *Nature.* 2012; 489:309–312. [PubMed: 22885698]
3. Burger JA, Ghia P, Rosenwald A, Caligaris-Cappio F. The microenvironment in mature B-cell malignancies: a target for new treatment strategies. *Blood.* 2009; 114:3367–3375. [PubMed: 19636060]
4. Herishanu Y, Perez-Galan P, Liu D, Biancotto A, Pittaluga S, Vire B, et al. The lymph node microenvironment promotes B-cell receptor signaling, NF-kappaB activation, and tumor proliferation in chronic lymphocytic leukemia. *Blood.* 2011; 117:563–574. [PubMed: 20940416]

5. Dal Bo M, Tissino E, Benedetti D, Caldana C, Bomben R, Del Poeta G, et al. Microenvironmental Interactions in Chronic Lymphocytic Leukemia: The Master Role of CD49d. *Semin Hematol.* 2014; 51:168–176. [PubMed: 25048781]
6. Stevenson FK, Forconi F, Packham G. The meaning and relevance of B-cell receptor structure and function in chronic lymphocytic leukemia. *Semin Hematol.* 2014; 51:158–167. [PubMed: 25048780]
7. Wiestner A. Emerging role of kinase-targeted strategies in chronic lymphocytic leukemia. *Blood.* 2012; 120:4684–4691. [PubMed: 22875912]
8. Burger JA, Chiorazzi N. B cell receptor signaling in chronic lymphocytic leukemia. *Trends Immunol.* 2013; 34:592–601. [PubMed: 23928062]
9. Humphries LA, Dangelmaier C, Sommer K, Kipp K, Kato RM, Griffith N, et al. Tec kinases mediate sustained calcium influx via site-specific tyrosine phosphorylation of the phospholipase Cgamma Src homology 2-Src homology 3 linker. *J Biol Chem.* 2004; 279:37651–37661. [PubMed: 15184383]
10. Kil LP, de Bruijn MJ, van Hulst JA, Langerak AW, Yuvaraj S, Hendriks RW. Bruton's tyrosine kinase mediated signaling enhances leukemogenesis in a mouse model for chronic lymphocytic leukemia. *American journal of blood research.* 2013; 3:71–83. [PubMed: 23359016]
11. Woyach JA, Bojnik E, Ruppert AS, Stefanovski MR, Goettl VM, Smucker KA, et al. Bruton's tyrosine kinase (BTK) function is important to the development and expansion of chronic lymphocytic leukemia (CLL). *Blood.* 2014; 123:1207–1213. [PubMed: 24311722]
12. Advani RH, Buggy JJ, Sharman JP, Smith SM, Boyd TE, Grant B, et al. Bruton tyrosine kinase inhibitor ibrutinib (PCI-32765) has significant activity in patients with relapsed/refractory B-cell malignancies. *J Clin Oncol.* 2013; 31:88–94. [PubMed: 23045577]
13. Byrd JC, Furman RR, Coutre SE, Flinn IW, Burger JA, Blum KA, et al. Targeting BTK with ibrutinib in relapsed chronic lymphocytic leukemia. *N Engl J Med.* 2013; 369:32–42. [PubMed: 23782158]
14. Farooqui MZ, Valdez J, Martyr S, Aue G, Saba N, Niemann CU, et al. Ibrutinib for previously untreated and relapsed or refractory chronic lymphocytic leukaemia with TP53 aberrations: a phase 2, single-arm trial. *Lancet Oncol.* 2014; 16:169–176. [PubMed: 25555420]
15. Byrd JC, Brown JR, O'Brien S, Barrientos JC, Kay NE, Reddy NM, et al. Ibrutinib versus Ofatumumab in Previously Treated Chronic Lymphoid Leukemia. *N Engl J Med.* 2014; 371:213–223. [PubMed: 24881631]
16. Herman SE, Niemann CU, Farooqui M, Jones J, Mustafa RZ, Lipsky A, et al. Ibrutinib-induced lymphocytosis in patients with chronic lymphocytic leukemia: correlative analyses from a phase II study. *Leukemia.* 2014; 28:2188–2196. [PubMed: 24699307]
17. Herishanu Y, Katz BZ, Lipsky A, Wiestner A. Biology of chronic lymphocytic leukemia in different microenvironments: clinical and therapeutic implications. *Hematol Oncol Clin North Am.* 2013; 27:173–206. [PubMed: 23561469]
18. de Rooij MF, Kuil A, Geest CR, Eldering E, Chang BY, Buggy JJ, et al. The clinically active BTK inhibitor PCI-32765 targets B-cell receptor- and chemokine-controlled adhesion and migration in chronic lymphocytic leukemia. *Blood.* 2012; 119:2590–2594. [PubMed: 22279054]
19. Ponader S, Chen SS, Buggy JJ, Balakrishnan K, Gandhi V, Wierda WG, et al. The Bruton tyrosine kinase inhibitor PCI-32765 thwarts chronic lymphocytic leukemia cell survival and tissue homing in vitro and in vivo. *Blood.* 2012; 119:1182–1189. [PubMed: 22180443]
20. Dal Bo M, Bomben R, Zucchetto A, Del Poeta G, Gaidano G, Deaglio S, et al. Microenvironmental interactions in chronic lymphocytic leukemia: hints for pathogenesis and identification of targets for rational therapy. *Curr Pharm Des.* 2012; 18:3323–3334. [PubMed: 22591383]
21. Zucchetto A, Vaisitti T, Benedetti D, Tissino E, Bertagnolo V, Rossi D, et al. The CD49d/CD29 complex is physically and functionally associated with CD38 in B-cell chronic lymphocytic leukemia cells. *Leukemia.* 2012; 26:1301–1312. [PubMed: 22289918]
22. Bulian P, Shanafelt TD, Fegan C, Zucchetto A, Cro L, Nuckel H, et al. CD49d Is the Strongest Flow Cytometry-Based Predictor of Overall Survival in Chronic Lymphocytic Leukemia. *J Clin Oncol.* 2014; 32:897–904. [PubMed: 24516016]

23. Pepper C, Buggins AG, Jones CH, Walsby EJ, Forconi F, Pratt G, et al. Phenotypic heterogeneity in IGHV-mutated CLL patients has prognostic impact and identifies a subset with increased sensitivity to BTK and PI3Kdelta inhibition. *Leukemia*. 2015; 29:744–747. [PubMed: 25349153]
24. Burger M, Hartmann T, Krome M, Rawluk J, Tamamura H, Fujii N, et al. Small peptide inhibitors of the CXCR4 chemokine receptor (CD184) antagonize the activation, migration, and antiapoptotic responses of CXCL12 in chronic lymphocytic leukemia B cells. *Blood*. 2005; 106:1824–1830. [PubMed: 15905192]
25. Herman SE, Sun X, McAuley EM, Hsieh MM, Pittaluga S, Raffeld M, et al. Modeling tumor-host interactions of chronic lymphocytic leukemia in xenografted mice to study tumor biology and evaluate targeted therapy. *Leukemia*. 2013; 27:1769–1773. [PubMed: 23385377]
26. Herman SE, Barr PM, McAuley EM, Liu D, Wiestner A, Friedberg JW. Fostamatinib inhibits B-cell receptor signaling, cellular activation and tumor proliferation in patients with relapsed and refractory chronic lymphocytic leukemia. *Leukemia*. 2013; 27:1769–1773. [PubMed: 23385377]
27. Jalkanen S, Jalkanen M. Lymphocyte CD44 binds the COOH-terminal heparin-binding domain of fibronectin. *J Cell Biol*. 1992; 116:817–825. [PubMed: 1730778]
28. To WS, Midwood KS. Plasma and cellular fibronectin: distinct and independent functions during tissue repair. *Fibrogenesis & tissue repair*. 2011; 4:21. [PubMed: 21923916]
29. Spaargaren M, Beuling EA, Rurup ML, Meijer HP, Klok MD, Middendorp S, et al. The B cell antigen receptor controls integrin activity through Btk and PLCgamma2. *J Exp Med*. 2003; 198:1539–1550. [PubMed: 14610042]
30. de Gorter DJ, Beuling EA, Kersseboom R, Middendorp S, van Gils JM, Hendriks RW, et al. Bruton's tyrosine kinase and phospholipase Cgamma2 mediate chemokine-controlled B cell migration and homing. *Immunity*. 2007; 26:93–104. [PubMed: 17239630]
31. Hurley JH, Newton AC, Parker PJ, Blumberg PM, Nishizuka Y. Taxonomy and function of C1 protein kinase C homology domains. *Protein Sci*. 1997; 6:477–480. [PubMed: 9041654]
32. Friedberg JW, Sharman J, Sweetenham J, Johnston PB, Vose JM, Lacasce A, et al. Inhibition of Syk with fostamatinib disodium has significant clinical activity in non-Hodgkin lymphoma and chronic lymphocytic leukemia. *Blood*. 2010; 115:2578–2585. [PubMed: 19965662]
33. Herman SE, Gordon AL, Hertlein E, Ramanunni A, Zhang X, Jaglowski S, et al. Bruton tyrosine kinase represents a promising therapeutic target for treatment of chronic lymphocytic leukemia and is effectively targeted by PCI-32765. *Blood*. 2011; 117:6287–6296. [PubMed: 21422473]
34. Srichai, M.; Zent, R. Integrin Structure and Function. In: Zent, R.; Pozzi, A., editors. *Cell-Extracellular Matrix Interactions in Cancer*. New York: Springer; 2010. p. 19-41.
35. Arana E, Harwood NE, Batista FD. Regulation of integrin activation through the B-cell receptor. *J Cell Sci*. 2008; 121:2279–2286. [PubMed: 18596256]
36. Calissano C, Damle RN, Marsilio S, Yan XJ, Yancopoulos S, Hayes G, et al. Intracлонаl complexity in chronic lymphocytic leukemia: fractions enriched in recently born/divided and older/quiescent cells. *Mol Med*. 2011; 17:1374–1382. [PubMed: 21968788]
37. Walsby E, Buggins A, Devereux S, Jones C, Pratt G, Brennan P, et al. Development and characterization of a physiologically relevant model of lymphocyte migration in chronic lymphocytic leukemia. *Blood*. 2014; 123:3607–3617. [PubMed: 24637360]
38. de la Fuente MT, Casanova B, Garcia-Gila M, Silva A, Garcia-Pardo A. Fibronectin interaction with alpha4beta1 integrin prevents apoptosis in B cell chronic lymphocytic leukemia: correlation with Bcl-2 and Bax. *Leukemia*. 1999; 13:266–274. [PubMed: 10025901]
39. Buggins AG, Pepper C, Patten PE, Hewamana S, Gohil S, Moorhead J, et al. Interaction with vascular endothelium enhances survival in primary chronic lymphocytic leukemia cells via NF-kappaB activation and de novo gene transcription. *Cancer Res*. 2010; 70:7523–7533. [PubMed: 20736369]
40. Buchner M, Baer C, Prinz G, Dierks C, Burger M, Zenz T, et al. Spleen tyrosine kinase inhibition prevents chemokine- and integrin-mediated stromal protective effects in chronic lymphocytic leukemia. *Blood*. 2010; 115:4497–4506. [PubMed: 20335218]
41. Herman SE, Mustafa RZ, Gyamfi JA, Pittaluga S, Chang S, Chang B, et al. Ibrutinib inhibits BCR and NF-kappaB signaling and reduces tumor proliferation in tissue-resident cells of patients with CLL. *Blood*. 2014; 123:3286–3295. [PubMed: 24659631]

42. Wodarz D, Garg N, Komarova NL, Benjamini O, Keating MJ, Wierda WG, et al. Kinetics of chronic lymphocytic leukemia (CLL) cells in tissues and blood during therapy with the BTK inhibitor ibrutinib. *Blood*. 2014
43. Andritsos, LBJC.; Jones, JA.; Hewes, B.; Kipps, TJ.; Hsu, FJ.; Burger, JA. American Society of Hematology; 2010; *Blood*. Orlando, FL: 2010. Preliminary Results From A Phase I Dose Escalation Study to Determine the Maximum Tolerated Dose of Plerixafor In Combination with Rituximab In Patients with Relapsed Chronic Lymphocytic Leukemia. Abstract 772.
44. Rettig MP, Ansstas G, DiPersio JF. Mobilization of hematopoietic stem and progenitor cells using inhibitors of CXCR4 and VLA-4. *Leukemia*. 2012; 26:34–53. [PubMed: 21886173]
45. Burger JA, Peled A. CXCR4 antagonists: targeting the microenvironment in leukemia and other cancers. *Leukemia*. 2009; 23:43–52. [PubMed: 18987663]
46. Uy GL, Rettig MP, Motabi IH, McFarland K, Trinkaus KM, Hladnik LM, et al. A phase 1/2 study of chemosensitization with the CXCR4 antagonist plerixafor in relapsed or refractory acute myeloid leukemia. *Blood*. 2012; 119:3917–3924. [PubMed: 22308295]
47. O'Brien, SMBJC.; Flinn, IW.; Barr, PM.; Burger, JA.; Navarro, T.; James, DF.; Hedrick, E.; Friedberg, JW.; Brown, JR. Combination of the Bruton's tyrosine kinase (BTK) inhibitor PCI-32765 with bendamustine (B)/rituximab (R) (BR) in patients (pts) with relapsed/refractory (R/R) chronic lymphocytic leukemia (CLL): Interim results of a phase Ib/II study. ASCO annual meeting; 2012; Chicago, IL. 2012.
48. Barrientos JC, Barr PM, Flinn I, Burger JA, Salman Z, Clow F, et al. Ibrutinib In Combination With Bendamustine and Rituximab Is Active and Tolerable In Patients With Relapsed/Refractory CLL/SLL: Final Results Of a Phase 1b Study. *Blood*. 2013; 122:525.
49. Burger JA, Keating MJ, Wierda WG, Hartmann E, Hoellenriegel J, Rosin NY, et al. Safety and activity of ibrutinib plus rituximab for patients with high-risk chronic lymphocytic leukaemia: a single-arm, phase 2 study. *Lancet Oncol*. 2014; 15:1090–1089. [PubMed: 25150798]
50. Jaglowski, SMJJA.; Flynn, JM.; Andritsos, LA.; Maddocks, KJ.; Woyach, JA.; Blum, KA.; Grever, MR.; Geyer, SM.; Heerema, NA.; Lozanski, G.; Stefanos, M.; Hall, N.; Nagar, V.; Munneke, B.; West, JS.; Neuenburg, J.; James, DF.; Johson, AJ.; Byrd, JC. A phase 1b/2 study evaluating activity and tolerability of the BTK inhibitor ibrutinib in combination with ofatumumab in patients with chronic lymphocytic leukemia/small lymphocytic lymphoma (CLL/SLL) and related diseases. ASCO Annual Meeting; 2014; Chicago, Illinois. 2014. 2014.

Statement of Translational Relevance

Ibrutinib, as well as other BCR-directed kinase inhibitors, leads to a transient, treatment-induced lymphocytosis. The increase in CLL cells in the blood develops within hours of the first drug dose due to an efflux of cells out of the lymphoid tissues. Given that redistribution-lymphocytosis is a characteristic observation when treating CLL with ibrutinib, we sought to better understand the underlying biological mechanism by evaluating the *in vivo* effect of ibrutinib on the ability of CLL cells to migrate and adhere to stromal cells and components of the extracellular matrix. While we found an overall reduction in both migration and adhesion, only the ability of CLL cells to adhere to fibronectin was rapidly and almost completely inhibited by ibrutinib in all patients evaluated. The adhesion defect induced by ibrutinib was VLA-4 dependent, providing a mechanistic explanation for the treatment-induced lymphocytosis and suggesting a role for ibrutinib in disrupting CD49d-dependent pro-survival signals.

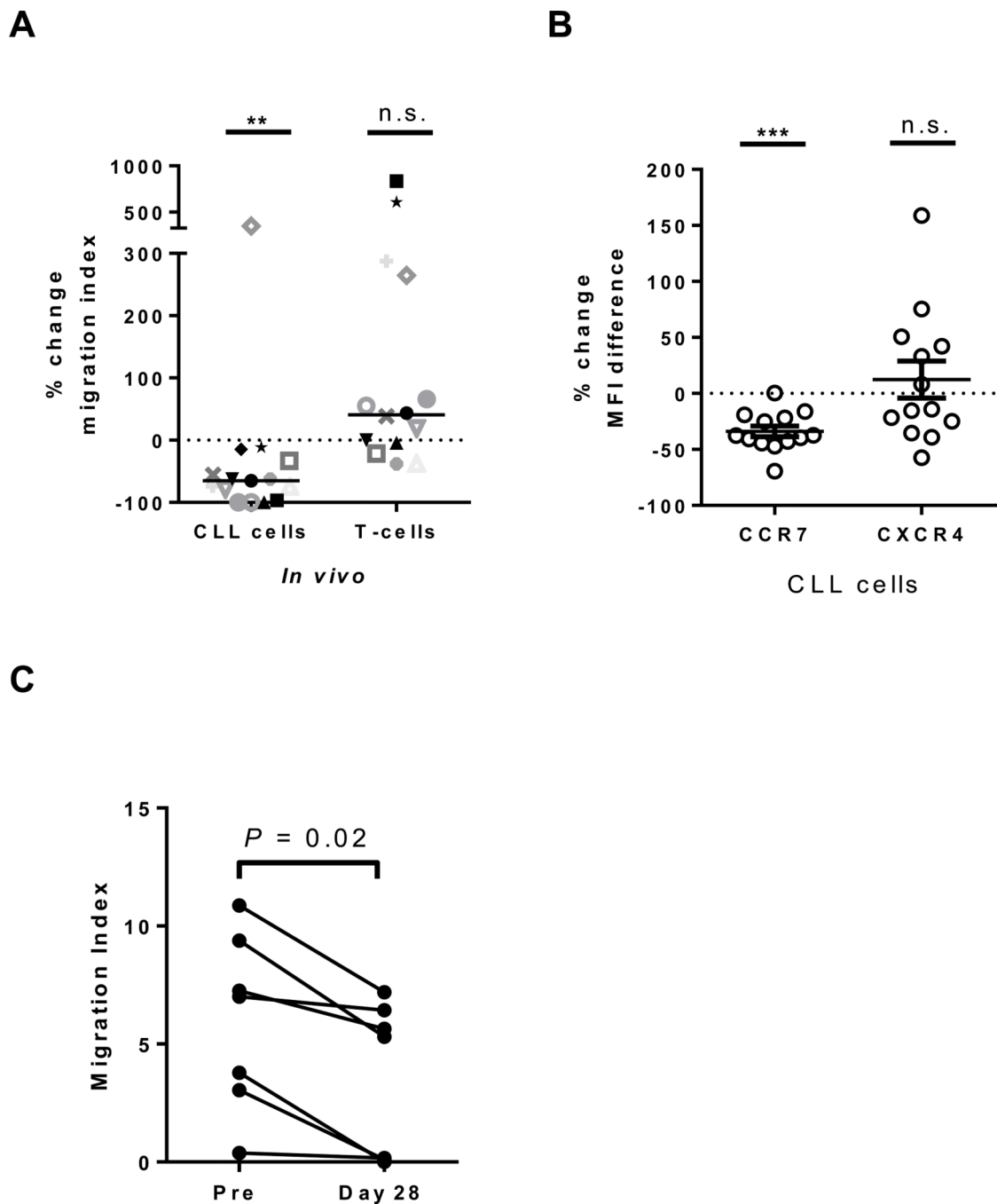


Figure 1. Effect of ibrutinib on cell migration. A, The percent change in cell migration of CLL PBMCs (n=15) collected on day 28 of ibrutinib compared to pre-treatment towards CXCL12/CCL19 is shown. Patient symbols correspond to those used in Supplemental Figure S1A. B, The percent change in expression of CCR7 and CXCR4 on CLL PBMCs (n=13) collected on day 28 of ibrutinib compared to pre-treatment. C, The magnitude of CLL cell migration towards patient matched bone marrow supernatant obtained pre-treatment is shown for CLL cells collected from the peripheral blood at baseline (Pre) and

on study day 28. Each line represents the reduction in migration potential for one patient (n=7). All Statistics were determined by a Wilcoxon matched pairs test, ** $P < 0.01$, *** $P < 0.001$.

Author Manuscript

Author Manuscript

Author Manuscript

Author Manuscript

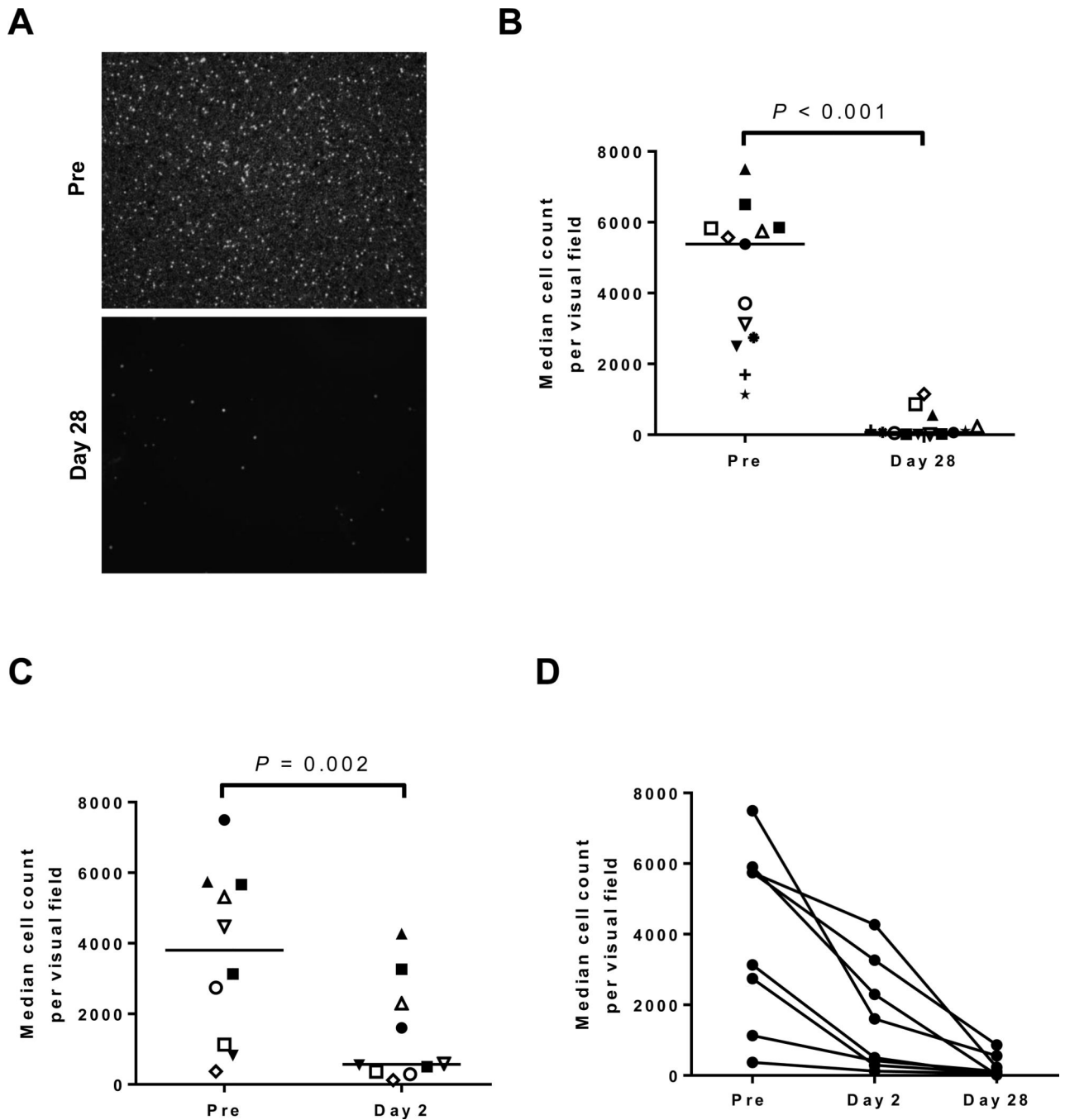
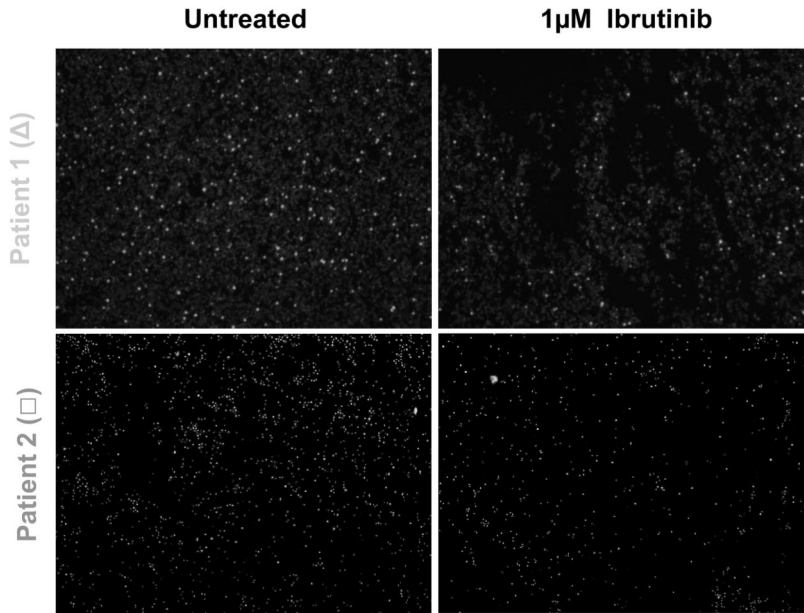


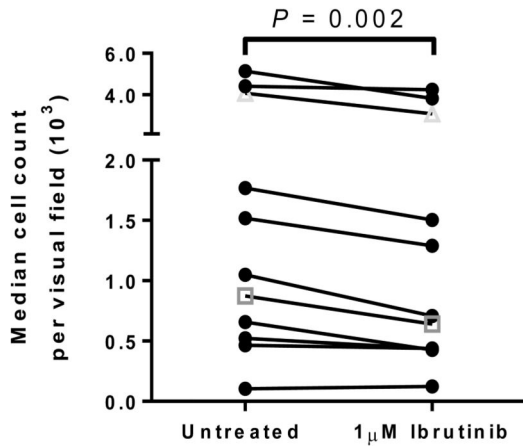
Figure 2. Effect of ibrutinib on cellular adhesion to fibronectin. A, Representative microphotographs showing the number of CLL PBMCs adhered to a fibronectin coated plate after 1 hour incubation; top panel, sample collected pre-treatment (Pre), bottom panel, sample collected on study day 28 from the same patient. B, The number of adherent cells per visual field is shown for PBMCs obtained pre-treatment and after 28 days on ibrutinib (n=13). Each symbol represents a different patient, lines represent the median. C, The number of adherent cells per visual field is shown for PBMCs obtained pre-treatment and after 24 hours on

ibrutinib (n=10). Each symbol represents a different patient, lines represent the median. D, The median cell count per visual field is shown for PBMCs obtained pre-treatment (Pre), on day 2, and day 28. Lines connect data points from sequential samples of the same patient (n=8). All Statistics were determined by a Wilcoxon matched pairs test.

A



B



C

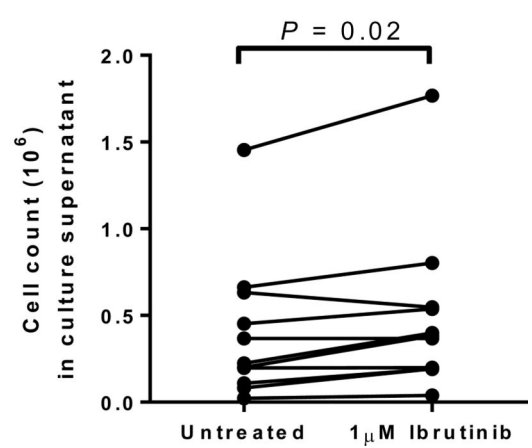


Figure 3.

Release of adhered cells by ibrutinib *in vitro*. A, Microphotographs show results from two representative patients. CLL PBMCs were adhered to fibronectin coated plates that were left untreated or incubated for 1 hour with ibrutinib. B, The median cell count per visual field on untreated and ibrutinib treated plates is shown. Lines connect results obtained with cells from the same patient (n=11). Symbols correspond to the representative patients depicted in panel A. C, The number of CLL PBMCs released from the fibronectin coated plate into the media after 1 hour of incubation with ibrutinib compared to control is shown. Lines connect

results obtained with cells from the same patient (n=11). All Statistics were determined by a Wilcoxon matched pairs test.

Author Manuscript

Author Manuscript

Author Manuscript

Author Manuscript

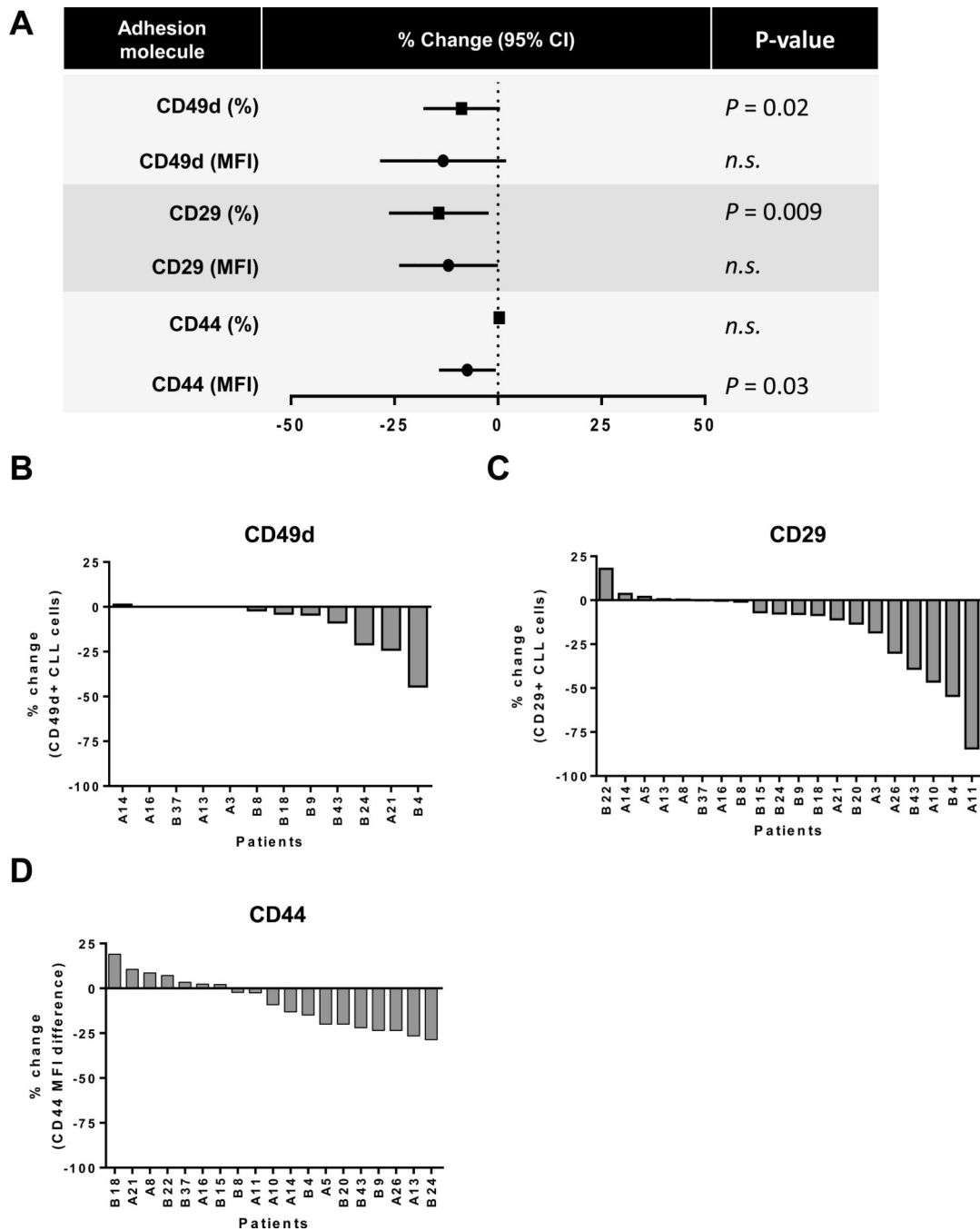


Figure 4.

In vivo effect of ibrutinib on the expression of adhesion molecules that bind fibronectin. A, Shown is the reduction in the expression of common adhesion molecules that bind to fibronectin, both as the proportion of CLL cells, percent of cells expressing each molecule above isotype control (squares), and the respective mean fluorescence intensity (MFI; circles). Symbols represent the mean; lines represent the 95% CI. *P* values determined by a Wilcoxon matched pairs test. B, Waterfall plots depicting the percent change in cells expressing CD49d, only for patients expressing CD49d at baseline (n=12) on day 28

compared to baseline. C, Waterfall plots depicting the percent change in cells expressing CD29 (n=20) on day 28 compared to baseline. D, Waterfall plot depicting the percent change in MFI for CD44 (n=19) on day 28 compared to baseline.

Author Manuscript

Author Manuscript

Author Manuscript

Author Manuscript

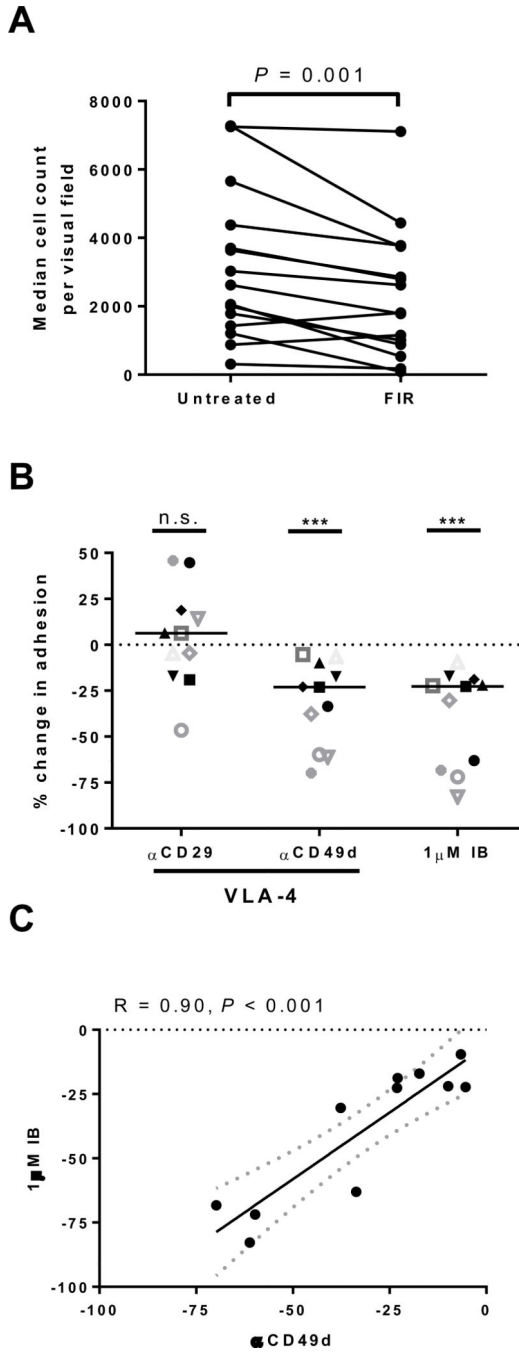


Figure 5. The role of BTK and VLA-4 in CLL cell adhesion to fibronectin. **A**, The median count of cells adhering to fibronectin coated plates per visual field is shown pre-treatment (Pre) and after 1 hour of incubation with 500nM fimategrast (FIR; VLA-4 antagonist). Lines connect results obtained with cells from the same patient (n=15), *P* value by Wilcoxon matched pairs test. **B**, The percent change in cell adhesion normalized to untreated control is shown for samples (n=11) treated for 1 hour with blocking antibodies against either CD29 (α CD29) or CD49d (α CD49d) the two components of VLA-4, or with 1 μ M ibrutinib (IB). Each symbol

represents a different patient. Lines represent median. *P* value determined by a Wilcoxon matched pairs test: *** $P < 0.001$. *C*, Pearson's correlation of the reduction in cell adhesion by ibrutinib (IB) and α CD49d. Each circle represents a different patient ($n=11$); dotted lines represent 95% confidence interval.

Author Manuscript

Author Manuscript

Author Manuscript

Author Manuscript

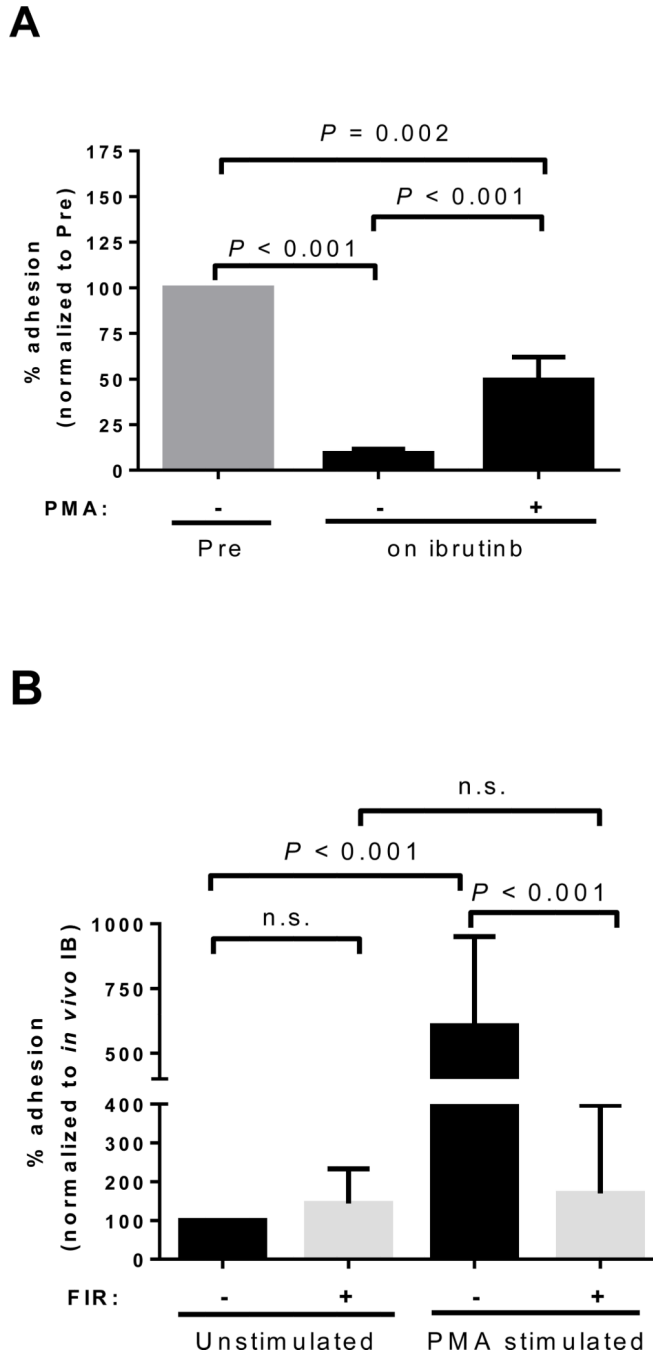


Figure 6. Reversibility of the ibrutinib-induced adhesion defect. A, Cells obtained from patients pre-treatment (Pre) or on ibrutinib were left unstimulated or stimulated with PMA for 1 hour. Shown is the mean (\pm SEM) percent reduction in adhesion normalized to pre-treatment samples (n=12). B, Adhesion of CLL PBMCs sampled during ibrutinib treatment analyzed under four different treatment conditions; cells were left unstimulated or stimulated with PMA, and in each of these two conditions cells were incubated with or without the addition of firtategrast (FIR; VLA-4 antagonist). Data is normalized to cells without PMA and

without FIR, representing the effect of ibrutinib (IB) *in vivo*. Shown is the mean (\pm SEM) percent change in cell adhesion (n=11). All *P* values were determined by a Wilcoxon matched pairs test.

Author Manuscript

Author Manuscript

Author Manuscript

Author Manuscript